Ring rolling

This example illustrates the use of adaptive meshing in a two-dimensional rolling simulation. Results are compared to those obtained using a pure Lagrangian approach.

This page discusses:

Products: Abaqus/Explicit

Problem description

Ring rolling is a specialized process typically used to manufacture parts with revolved geometries such as bearings. The three-dimensional rolling setup usually includes a freely mounted, idle roll; a continuously rotating driver roll; and guide rolls in the rolling plane. Transverse to the rolling plane, conical rolls are used to stabilize the ring and provide a forming surface in the out-of-plane direction. In this example a two-dimensional, plane stress idealization is used that ignores the effect of the conical rolls. A schematic diagram of the ring and the surrounding tools is shown in Figure 1.

The driver roll has a diameter of 680 mm, and the idle and guide rolls have diameters of 102 mm. The ring has an initial inner diameter of 127.5 mm and a thickness of 178.5 mm. The idle and driver rolls are arranged vertically and are in contact with the inner and outer surfaces of the ring, respectively. The driver roll is rotated around its stationary axis, while the idle roll is moved vertically downward at a specified feed rate. For this simulation the x–y motion of the guide rolls is determined *a priori* and is prescribed so that the rolls remain in contact with the ring throughout the analysis but do not exert appreciable force on it. In practice the guide rolls are usually connected through linkage systems, and their motion is a function of both force and displacement.

The ring is meshed with CPS4R elements, as shown in Figure 2. The ring is steel and is modeled as a von Mises elastic-plastic material with a Young's modulus of 150 GPa, an initial yield stress of 168.7 MPa, and a constant hardening slope of 884 MPa. The Poisson's ratio is 0.3; the density is 7800 kg/m^3.

The analysis is run so that the ring completes approximately 20 revolutions (16.5 seconds). The rigid rolls are modeled as analytical rigid surfaces using connected line segments. The driver roll is rotated at a constant angular velocity of 3.7888 rad/sec about the z-axis, while the idle roll has a constant feed rate of 4.9334 mm/sec and is free to rotate about the z-axis. All other degrees of

freedom for the driver and idle rolls are constrained. A friction coefficient of 0.5 is defined at the blank-idle roll and blank-drive roll interfaces. Frictionless contact is used between the ring and guide rolls, and the rotation of the guide rolls is constrained since the actual guide rolls are free to rotate and exert negligible torque on the ring.

To obtain an economical solution, the masses of all elements in the ring are scaled by a factor of 2500. This scaling factor represents a reasonable upper limit on the mass scaling possible for this problem, above which significant inertial effects would be generated. Furthermore, since the two-dimensional model does not contain the conical rolls, the ring oscillates from side to side even under the action of the guide rolls. An artificial viscous pressure of 300 MPa sec/m is applied on the inner and outer surfaces of the ring to assist the guide rolls in preserving the circular shape of the ring. The pressure value was chosen by trial and error.

Adaptive meshing

A single adaptive mesh domain that incorporates the ring is defined. Contact surfaces on the ring are defined as sliding boundary regions (the default). Because of the large number of increments required to simulate 20 revolutions, the deformation per increment is very small. Therefore, the frequency of adaptive meshing is changed from the default of 10 to every 50 increments. The cost of adaptive meshing at this frequency is negligible compared to the underlying analysis cost.

Results and discussion

Figure 3 shows the deformed configuration of the ring after completing 20 revolutions with continuous adaptive meshing. High-quality element shapes and aspect ratios are maintained throughout the simulation. Figure 4 shows the deformed configuration of the ring when a pure Lagrangian simulation is performed. The pure Lagrangian mesh is distorted, especially at the inner radius where elements become skewed and very small in the radial direction.

Figure 5 and Figure 6 show time history plots for the *y*-component of reaction force on the idle roll and the reaction moment about the *z*-axis for the driver roll, respectively, for both the adaptive mesh and pure Lagrangian approaches. Although the final meshes are substantially different, the roll force and torque match reasonably well.

For both the adaptive and pure Lagrangian solutions the plane stress idealization used here results in very localized through-thickness straining at the inner and outer radii of the ring. This specific type of localized straining is unique to plane stress modeling and does not occur in ring rolling processes. It is also not predicted by a three-dimensional finite element model. If adaptivity is used and refined meshing is desired to capture strong gradients at the inner and outer extremities, the initially uniform mesh can be replaced with a graded mesh. Although not shown here, a graded mesh concentrates element refinement in areas of strong gradients. You can specify in the adaptive mesh controls that the initial mesh gradation should be preserved while distortions are reduced as the analysis evolves.

Input files

ale_ringroll_2d.inp

Analysis that uses adaptive meshing.

ale_ringroll_2dnode.inp

External file referenced by the adaptive mesh analysis.

ale_ringroll_2delem.inp

External file referenced by the adaptive mesh analysis.

guideamp.inp

External file referenced by the adaptive mesh analysis.

lag_ringroll_2d.inp

Lagrangian analysis.

Figures

Figure 1. Model geometry for the two-dimensional ring rolling analysis.

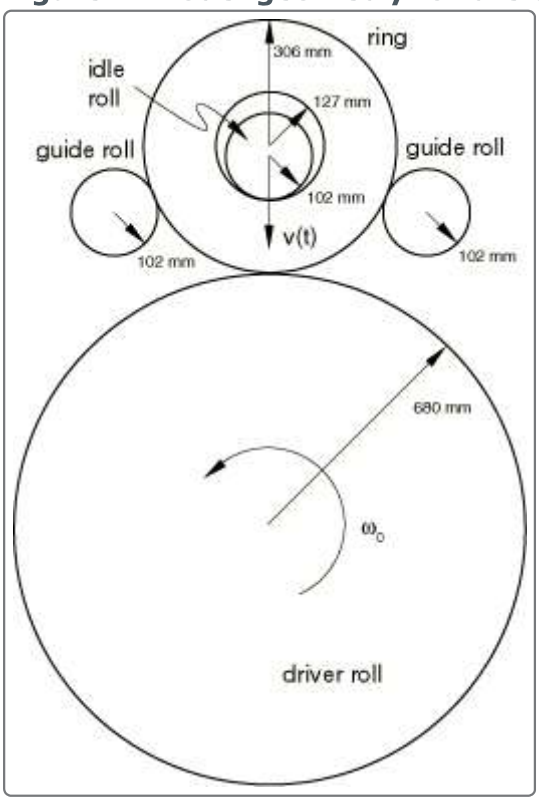

Figure 2. Initial mesh configuration.

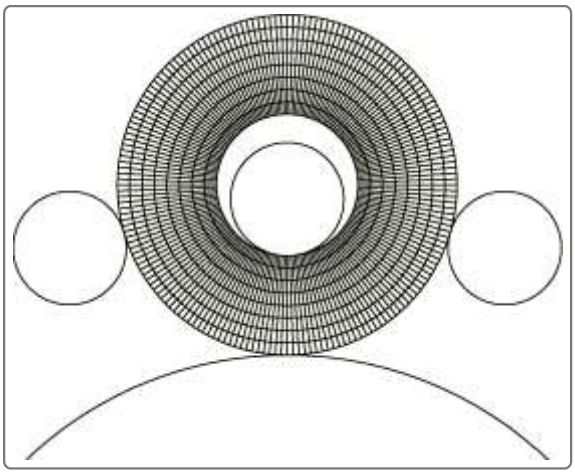

Figure 3. Deformed configuration after 20 revolutions using adaptive meshing.

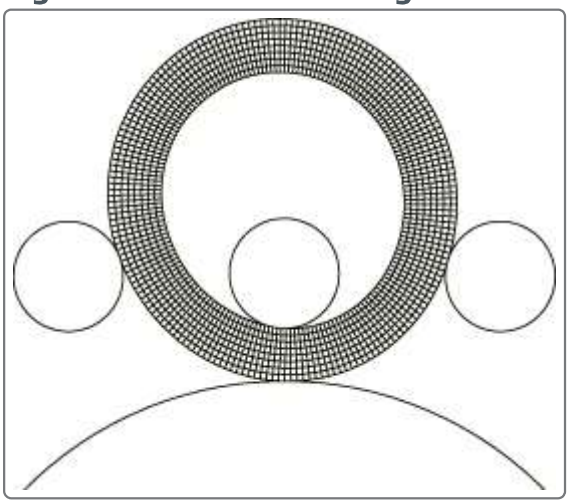

Figure 4. Deformed configuration after 20 revolutions using a pure Lagrangian approach.

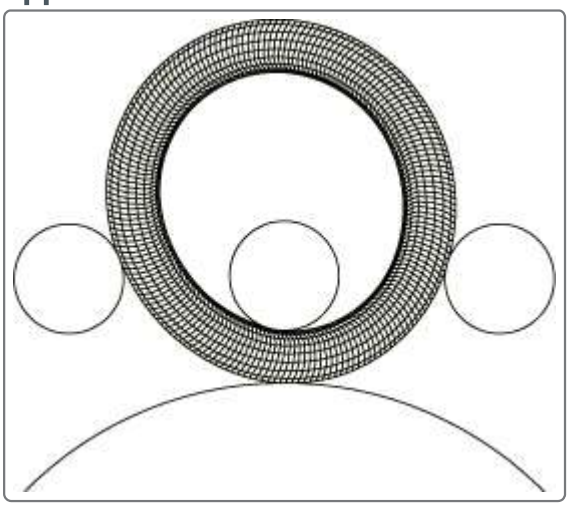

Figure 5. Time history of the reaction force in the *y*-direction for the idle roll.

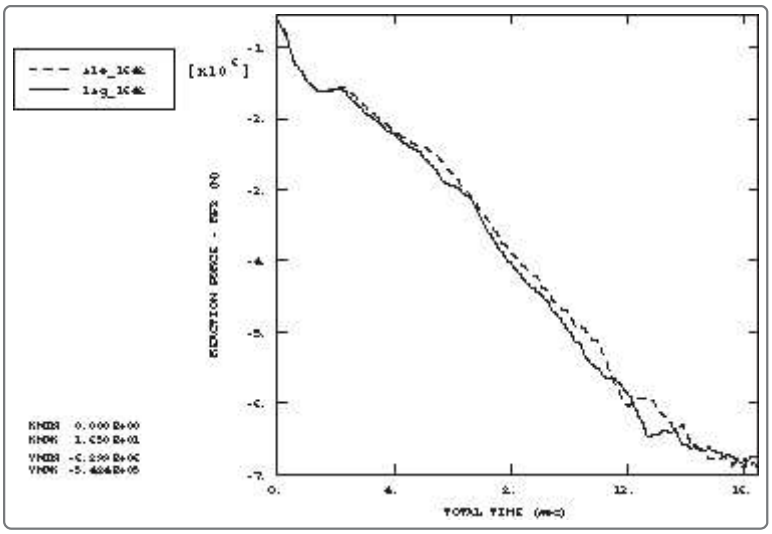

Figure 6. Time history of the reaction moment about the *z*-axis for the driver roll.